



## Rupture Tests with Reactor Pressure Vessel Head Models

Heli Talja, Heikki Keinänen, Ensio Hosio, Pekka H. Pankakoski, Klaus Rahka

VTT Industrial Systems, Espoo, Finland

### ABSTRACT

In the LISSAC project (LImit Strains in Severe ACCidents), partly funded by the EC Nuclear Fission and Safety Programme within the 5th Framework programme, an extensive experimental and computational research programme is conducted to study the stress state and size dependence of ultimate failure strains. The results are aimed especially to make the assessment of severe accident cases more realistic.

For the experiments in the LISSAC project a block of material of the German Biblis C reactor pressure vessel was available. As part of the project, eight reactor pressure vessel head models from this material (22 NiMoCr 3 7) were tested up to rupture at VTT. The specimens were provided by Forschungszentrum Karlsruhe (FzK).

These tests were performed under quasistatic pressure load at room temperature [1]. Two specimen sizes were tested and in half of the tests the specimens contain holes describing the control rod penetrations of an actual reactor pressure vessel head. These specimens were equipped with an aluminium liner. All six tests with the smaller specimen size were conducted successfully. In the test with the large specimen with holes, the behaviour of the aluminium liner material proved to differ from those of the smaller ones. As a consequence the experiment ended at the failure of the liner. The specimen without holes yielded results that were in very good agreement with those from the small specimens.

**KEY WORDS:** pressure vessel head model, pressure test, ultimate failure strain, size effect

### SPECIMENS AND EXPERIMENTAL SETUP

At VTT totally eight pressure vessel head models were tested. The specimens were delivered by FzK. Six first specimens were of the smaller size and for the other two, all dimensions were scaled by a factor of 5. Half of the specimens contained 73 equiaxial holes, describing the control rod penetrations in an actual reactor pressure vessel head.

For testing, the specimens were bolted to a rigid base plate using a fixture ring. The geometry of the specimen and the principle of the experimental setup are shown in Figure 1. The main dimensions of the smaller specimens are given in Table 1.

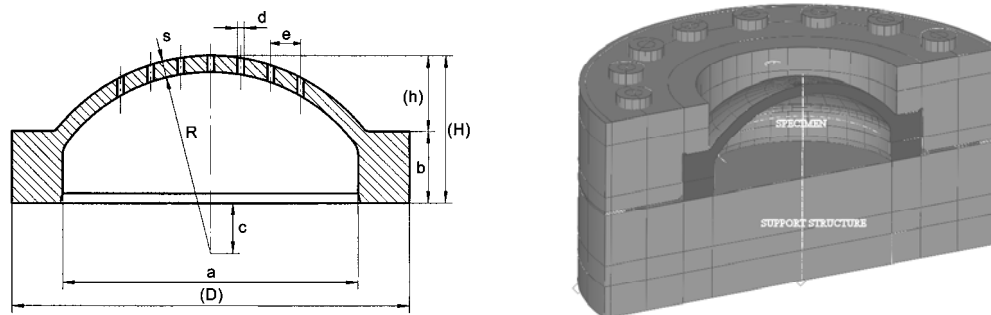


Fig. 1. Geometry of the small pressure vessel models with holes (left) and a schematic presentation of the experimental setup (right).

Table 1. Main dimensions of the smaller pressure vessel models.

a [mm]	R [mm]	s [mm]	h [mm]	b [mm]	d [mm]	e [mm]
90.6	55.6	5	23.2	22	2	4.6

## FE ANALYSES FOR PLANNING THE EXPERIMENTS

The experimental setup was carefully designed to withstand the failure pressure of the specimen, which was estimated to be around 1150 bar. The fixture system had to be very rigid, in order to ensure that no tightness problems would occur during the tests. Besides, no essential plastic deformations were allowed as the same fixture system had to be used in all tests with the same specimen size. Axisymmetric and three-dimensional finite element analyses were conducted to assess the behaviour of the experimental setup [2]. An important goal of the analyses was to help in assuring the reliability of the support structures and other facilities during the tests. Also, the specimen behaviour during the test was estimated.

As the dimensions of the fixture ring set limitations for the size and number of bolts, one of the main concerns in planning the test arrangements was the endurance of the bolts. On the other hand, due to the high expected failure pressure it was of paramount importance that no failure of test arrangements would occur during the tests. To ensure the proper functioning, both axisymmetric and three-dimensional finite element (FE) models were used in the computations (see Fig. 2). The 3D model enabled a more accurate estimation of the bolt behaviour. The elasto-plastic analyses were performed using Abaqus 5.8-14 finite element code [3]. Large strains and deformations were taken into account. In the analyses, mechanical properties documented by the LISSAC theoretical task group [4] were applied for the specimen.

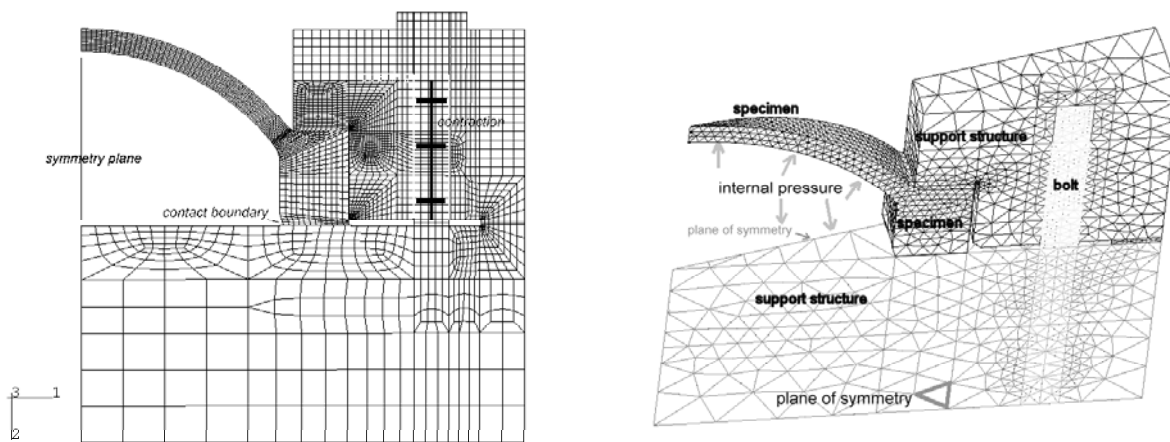


Fig. 2. Axisymmetric and three-dimensional finite element models used in the analyses [2]. The 3D model describes 1/32 of the whole geometry, corresponding to 32 bolts.

The main result of the analyses was that the maximum pressure would be about 1140 bar. So the bolts had to be able to carry a total load of 735 kN in the smaller size and 18 500 kN in the larger size. The results also indicated that no problems concerning to deformations and loss of integrity had to be expected.

## EXPERIMENTAL RESULTS

### Global results

During all tests the internal pressure and dome displacement were recorded up to failure. For small specimens also some strain measurements were performed. After the test, the minimum thickness values of the specimens without holes were measured.

For none of the eight performed tests, any interruptions or repetitions were necessary [1]. Seven tests were an immediate success. Although pressure loading is to be considered as a load controlled type loading, the test specimens strained in full control far beyond the strains at maximum pressure, as it was not possible to maintain the pressure level when the specimen started to yield rapidly. This was because the low displacement pump provided no accumulator to feed more water to compensate for the volume increase of the test piece. For the test with the large specimen with holes, however, the test ended prematurely before reaching failure of the specimen.

Table 2 compares the maximum pressure and related displacement values. It shows that the tests were very well reproducible. All tests with specimens without holes which were tested without liner, i.e. specimens EU1, ET1 and EW, gave maximum pressure values deviating only by  $\pm 0.2\%$  from the mean value of 115 MPa, which agrees well with the estimated ultimate load of 114 MPa. The scatter of the scaled maximum dome displacement values was 4.2% from the mean value 69.9% and, quite surprisingly, it was largest for the large specimen.

The three tests with small specimens with holes, EZ1, EY1 and FA1, also showed quite modest variation in the measured maximum pressures (0.7% of the mean value 110 MPa). The failure occurred at a scaled displacement of

28.2 % with a fairly small scatter of  $\pm 1.1$  %. According to Figure 6 this seems to correspond roughly to the ultimate load. In the test with the large specimen a pressure of 115 MPa, which seems to be smaller than the ultimate load, was reached. This different behaviour is most probably due to the lesser ductility of the liner material, compared to that of the small liners, although they were hoped to be identical and chosen with such expectations.

Table 2. Summary of main results from the pressure vessel head model tests.

Specimen	Diameter a [mm]	Holes	Liner	Max. pressure [MPa]	Max. displacement [% of dome height]
EU1	90.6			116	69.1
ET1	90.6			115	66.9
EV1	90.6		x	126	34.8
EZ1	90.6	x	x	111	27.9
EY1	90.6	x	x	109	28.3
FA1	90.6	x	x	109	28.4
EW	453			115	73.6
FB	453	x	x	117	17.3

Figure 3 shows the measured scaled dome displacement of each test as a function of pressure. The results seem to fall in four groups:

- 1) the tests with the specimens EU1, ET1 and EW without holes;
- 2) the test with the small specimen EV1 without holes which was tested with liner for comparison;
- 3) the three test results with small specimens EZ1, EY1 and FA1 with holes and
- 4) the test with the large specimen FB with holes.

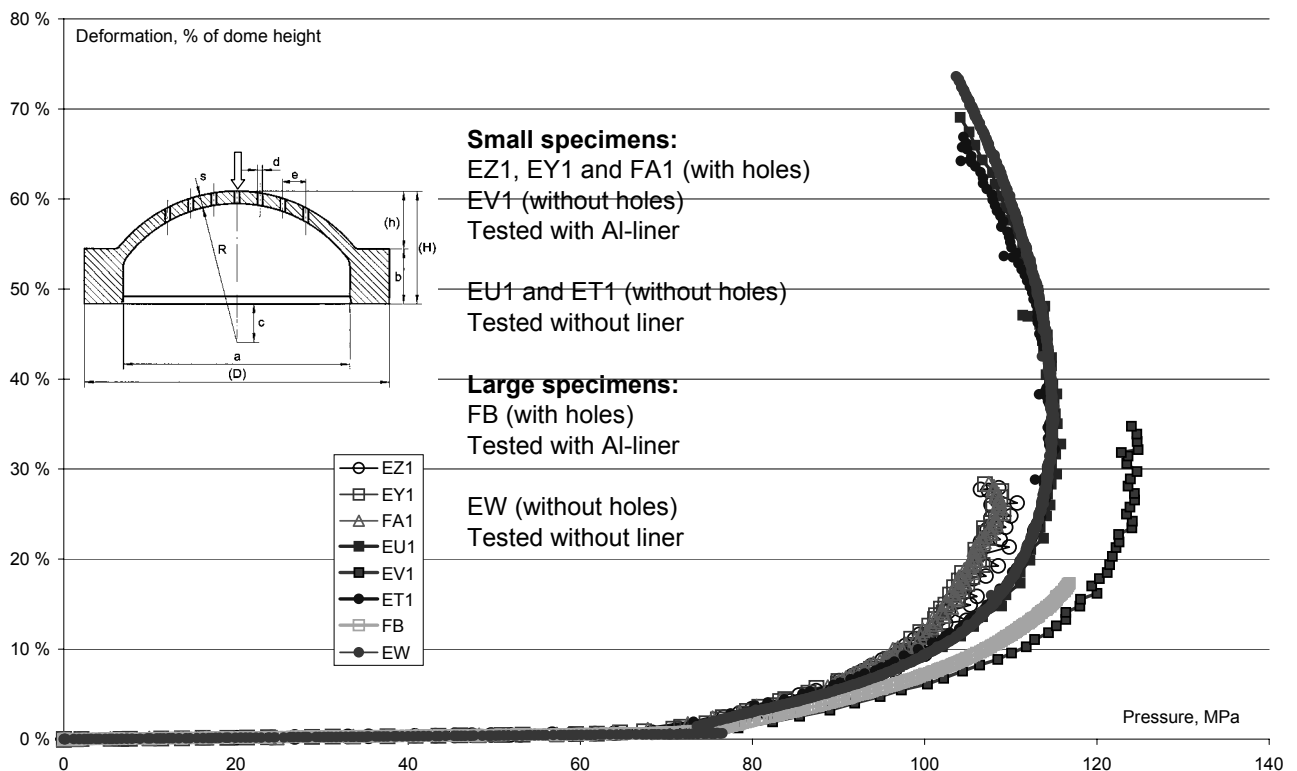


Fig. 3. Scaled dome displacement as a function of internal pressure.

Groups 2 and 4 contain both only one tests. Only in group 1 the tests continued beyond the strain at maximum pressure whereas this happened in none of the tests with a liner. Comparison of test groups 1 and 2 indicates that the liner increases the maximum pressure by about 10 MPa. The increase of maximum pressure appears to be an artefact due to the observed liner displacement during the test such that the strength of the lower ring of the liner increases the strength of the assembly.

Lowest maximum pressure values were obtained in the tests of group 3. The three tests in this group show very similar behaviour. The test with specimen FB (group 4) shows abnormal behaviour. The measured pressure values exceed clearly those in the corresponding tests with small specimens (group 3) while no difference was observed in the case of different specimen sizes without holes. Obviously the difference is thus connected to the behaviour of the liner.

**Normalisation for the effect of the holes and the liner**

Pressure-displacement records were normalised using global membrane stress and shape criteria and relative strength values for the steel specimens and the aluminium liners (Fig. 4). The test pressures were converted into steel net section membrane stress by adopting the usual sphere stress formula and factors for the liner thickness and strengths and the hole configuration.

The normalisation factors are:

for sphere stress  $\sigma = p \cdot R / 2s \cdot hf \cdot lf$ , where

- p = the internal pressure,
- R = dome inside radius and
- s = dome thickness =  $s_{st}$  below yielding  $R/2s = 5.56$ .

Further

- hf = hole factor = 1 for tests without holes and as given below for tests with holes and
- lf = liner factor = 1 for tests without liner and as given below for the liner effect.

Here the hole factor is

$hf = 1 / (1 - d/2e)$ , where  $d/2e = 2/9.2 = 10/46 = 0.217391$  for small and large specimen sizes and thus  $hf = 1.28$ .

The liner factor is

$lf = 1 / (1 + k \cdot Y_{S_{al}}/Y_{S_{st}} \cdot s_{al}/s_{st})$ , in which k is a fitting parameter and  $Y_{S_{al}}/Y_{S_{st}}$  the ratio of flow strengths aluminium/steel.

Here  $Y_{S_{al}}/Y_{S_{st}} = 234/500 = 0.47$  and  $s_{al}/s_{st}$  = thickness ratio liner/specimen

It was found that a value for  $k = 0.32$  for the smaller liner and  $k = 0.72$  for the larger produced consolidation of the different test records (taking aluminium yield stresses as 234 MPa for both small and large liners). A ratio of 1.13 is found for the "strengthening" effect of the holes using these net section membrane stress criteria, or a factor of  $1.13/1.28 = 0.884$  for the weakening effect of the holes on the global behaviour disregarding holes in the stress calculation. The consolidated curves are shown in Figure 4.

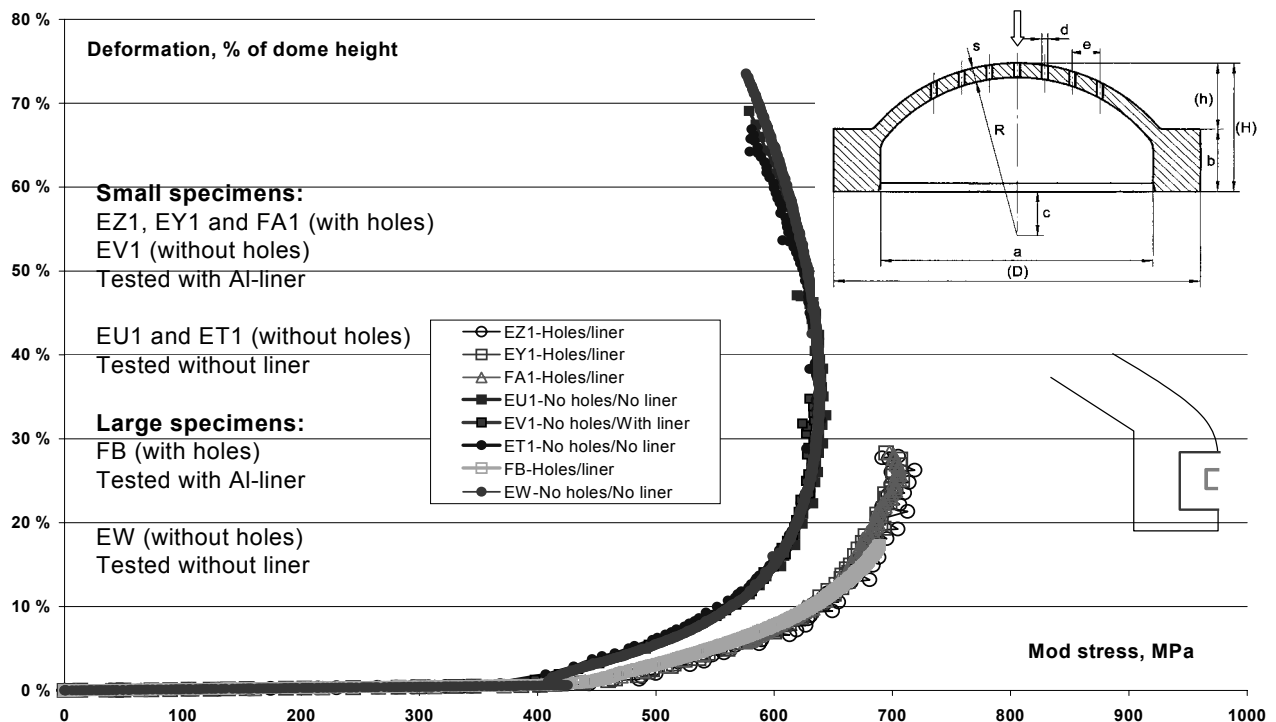


Fig. 4. Normalised membrane net stress for steel dome versus deformation of specimen.

The factor 1.13 on the net section strength is interesting because it is close to the ratio of fully plastic principal stress components for plane strain and equibiaxial strain thus proposing that the specimen ligaments between holes adopt a plane strain deformation mode whereas the dome without holes remains in the equibiaxial mode. This interpretation may be fortuitous, because the stress-strain concentration effect of the holes is neglected and the net section factor 1.28 is related to the less densely spaced 90 degree configuration prevailing in the dome centre.

The factors  $k$  for small and large liners differ by a factor slightly larger than 2 for several tentative reasons. The factor 2 can be deduced back to the retaining effect of the larger lower flange of the larger liner (relatively the O-ring groove is much smaller than in the small liner) preventing the larger liner to slip into the test specimen during pressurisation and causing the large liner into equibiaxial tension. The smaller liner was observed to slip into the steel dome during its deformation indicating that the small liner was forced into a "deep drawing" or pure shear deformation mode, which occurs at half the value of principal stress compared to equibiaxial tension. Hence the ratio around 2 between the factors  $k$  in the normalisation for the effect of small and large liners.

### Failure modes

Some specimens after the tests are shown in Figures 5 to 7. From the photos the failure modes of each specimen can be recognised.

Figure 5 shows a typical example of a tested small specimen without holes. The failure occurred as a leak at the uppermost part of the dome where the tensile strains are the highest. The effect of the liner reduced the failure strain and changed the mode of failure as is also demonstrated in Figure 5. As shown in Figure 6, the failure of the large specimen without holes (EW) was quite dramatic. A part of a size of about  $20 \times 15 \text{ cm}^2$  fragmented from the specimen. The related damage around the test set up was contained due to the precaution of testing upside down. Accordingly the loose part hit against a rigid floor and no serious damage was caused to the surroundings.

Figure 7 shows tested specimens with holes. On the left hand side is a typical example of a tested specimen with holes. Also the liner is shown. In this case the specimen broke along the first row of densely spaced holes, counting from the dome top. The test with the large specimen FB ended somewhat prematurely due to the failure of the liner. However, a similar yield pattern can already be recognised to develop which has caused the failure of the specimen EZ1.



Fig. 5. Specimens EU1 (left) and EV1 (right) after testing. Specimen EV1 was tested using a liner, which caused a premature failure by a failure mode deviating from those tested without liner.

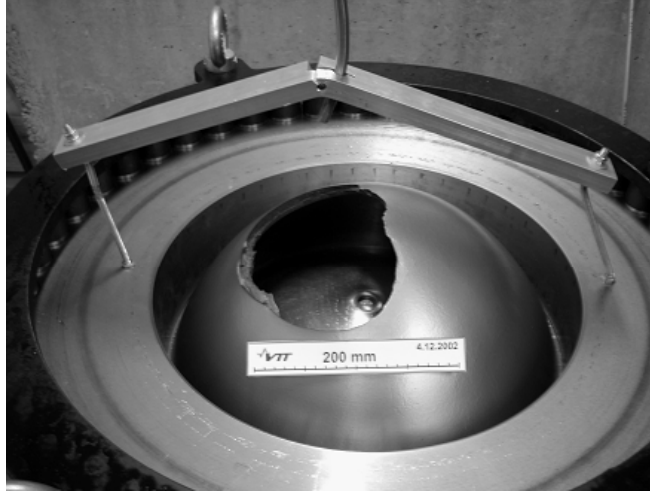


Fig. 6. Specimen EW (large size) after testing.

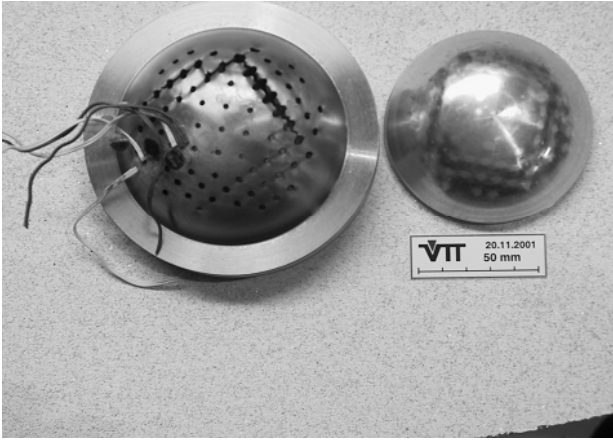


Fig. 7. Specimen EZ1 (small size) after testing, shown with the liner (left). Right: Specimen FB after testing. The test ended due to the failure of the liner.

### Local results

Thickness values were measured after the tests for the specimens without holes. The specimens with holes were sent for measurements to FzK. One of the small specimens without holes (ET1) had already been delivered to FzK. The measurements were actually performed for only two specimens.

The measured smallest thickness  $s_f$  of specimen EU1 was 2.0 mm and that of specimen EW was 10.4 mm. According to the method presented by Krieg and Dolensky [5], knowing the linear strain in the thickness direction,  $\varepsilon_s = -(s - s_f)/s$ , the true equivalent strain  $\varepsilon_{e,true}$  at failure can be calculated as

$$\varepsilon_{e,true} = \ln \left( 1 + \frac{2}{3} \left| \sqrt{\frac{1}{1 + \varepsilon_s}} - (1 + \varepsilon_s) \right| \right). \quad (1)$$

According to Eq. 1, the values of failure strains are 56.3 % and 58.1 % for the larger and smaller specimens, respectively. These values are practically identical. Other reasons why no conclusions concerning the size effect can be drawn based on these results are the small number of measurements and the rather limited accuracy of thickness measurement.

Failure strain calculation for tests with holes would require a method considering the strain concentration due to the holes.

## COMPARISON OF NUMERICAL AND EXPERIMENTAL RESULTS

Figure 8 shows a comparison of the results of the computations, which were aimed for planning of the experimental setup, to the measured ones for the specimens without holes. As the computed results were produced using a classical elastic-plastic material model without considering the softening effect due to damage, they reproduce only the ascending part of the load path. For this part the experimental results are predicted very well with both computations and the estimated maximum pressure is within 1% agreement with the experimental result.

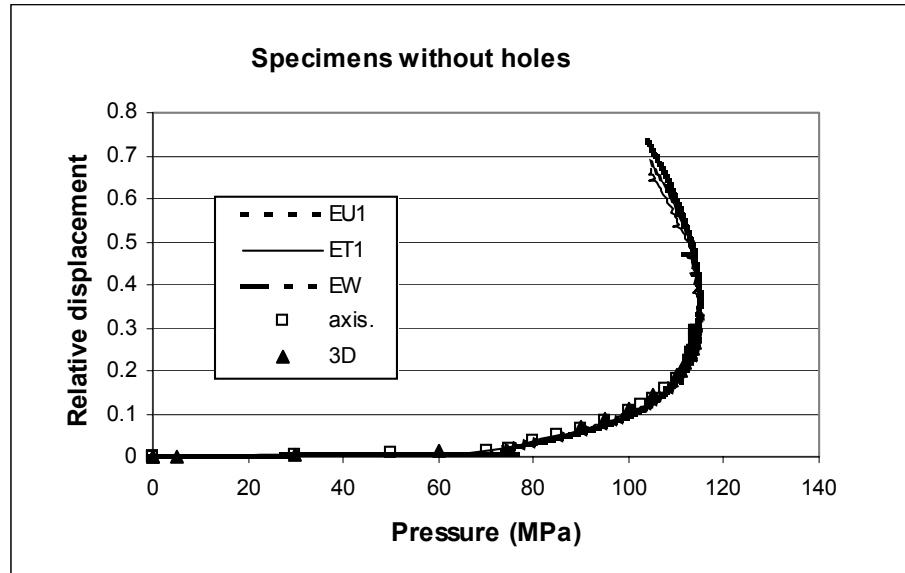


Fig. 8. Comparison of axisymmetric and three-dimensional FE results with the experimental ones for the specimens without holes.

The results of the pressure vessel head models have been used as a benchmark in the work package "Sample calculations for selected severe accident loads" of LISSAC. The tests using specimens without holes have been simulated by NRG, MPA and VTT. NRG has performed analyses with a non-local Gurson model and MPA with the Rousselier model. The results of the benchmark will be published later.

## SUMMARY AND CONCLUSIONS

In the auspices of the LISSAC project reactor pressure vessel head models from actual reactor pressure vessel material were tested up to rupture using internal pressure loading. The tests form a part of an extensive experimental programme where the stress state and size dependence of ultimate failure strains is studied.

At VTT specimens of two sizes were tested. The small specimens had an inside diameter of about 90 mm. The dimensions of the large specimens were scaled by a factor of 5. Half of the specimens contained a pattern of equiaxial holes describing the control rod penetrations. They were tested using an aluminium liner for tightening.

For the eight performed tests, interruptions or repetitions were unnecessary. Seven tests succeeded completely as planned. The maximum pressures varied between 1080 and 1250 bar. Although pressure loading is to be considered as a load controlled type loading, the tests ended only markedly after the maximum pressure, as it was not possible to maintain the pressure level when the specimen started to yield rapidly. The test with the large specimen with holes, however, ended prematurely before reaching the maximum pressure due to the failure of the liner. All other tests succeeded as planned and the test results were very well reproducible. Consolidation of test data was successful assuming different behaviours of large and small liners of the tests with holes. These differences were traced back mainly to geometrical differences of the two different liner sizes associated with the O-ring seal grooves used.

The test results presented here have been used as a benchmark in the work package "Sample calculations for selected severe accident loads" of LISSAC. The tests using specimens without holes have been simulated by NRG, MPA and VTT. The results of the benchmark will be published later.

## REFERENCES

1. Talja, H., Pankakoski, P., Hosio, E., Rahka, K. and Keinänen, H., Results of the LISSAC pressure vessel head model specimen tests. Research report TUO72-021094. VTT Industrial Systems, Espoo, 2003.
2. Keinänen, H. and Talja, H., Estimation of the limit load and strength of the LISSAC pressure test specimen. Research report VAL64-023620. VTT Industrial Systems, Espoo, 2002.
3. Abaqus 5.8. Hibbitt, Karlsson & Sorensen, Inc. 1998. Pawtucket, RI, USA.
4. LISSAC theoretical task group. Definition of stress strain law. Document: L\_MPA\_M01a.doc
5. Krieg, R. & Dolensky, B. 2002. Methods to determine the local failure strains for the broken LISSAC specimens. LISSAC project report SAM-LISSAC-D025.